Experimental and Numerical Study on Heat Transfer of Supercritical Water Flowing Upward in 2×2 Rod Bundles

M. Zhao[1, 3], H.Y.Gu[1] and X.Cheng[1, 3]
1: School of Nuclear Science and Engineering, Shanghai Jiao Tong University, Shanghai 200240, China
zhaomeng@sjtu.edu.cn ; guhanyang@sjtu.edu.cn; chengxu@sjtu.edu.cn

H.B.Li[2]
2: China Nuclear Power Technology Research Institute, China General Nuclear Power Group, Shenzhen 518026, China
lihongbo@cgnpc.com.cn

Q.R.Yang[3]
3: Institute of Fusion and Reactor Technology, Karlsruhe Institute of Technologies (KIT), Karlsruhe 76131, Germany
Yangqirui321@gmail.com

Abstract
Heat transfer characteristics of supercritical water flowing upward in 2×2 rod bundles have been investigated experimentally and numerically at conditions of pressure of 23-26MPa, mass flux of 450-1500kg/m^{2}s and heat flux of 0.4-1.5MW/ m^2. The diameter of each heated rod is 8mm, with pitch to diameter ratios 1.18 and 1.3. Heat transfer coefficient in 2×2 rod bundles was calculated and the effect of spacer grids was identified. The results show that heat transfer to supercritical water in 2×2 rod bundles is strongly dependant on mass flux, heat flux, pitch to diameter ratio and space grids. Moreover, a database of heat transfer in rod bundles, including the profile of circumferential temperature distribution, was established. It shows that the rod wall surface temperature closest to the center sub-channel is lower than any other place. Heat transfer is obviously enhanced by spacer grids. Numerical analysis based on Computational Fluid Dynamics (CFD) was also carried out and a deep insight of heat transfer enhancement was given.

Keywords:
Supercritical water, heat transfer, 2×2 rod bundles, spacer grids

1. Introduction

As one of the six Generation IV reactors selected by GIF, supercritical water cooled reactor (SCWR) has such advantages like higher thermal efficiency and system simplification [1]. However, in the frame of SCWR design, there are still many technical challenges, especially in the field of thermal hydraulics. The thermo-physical properties of supercritical water show

strong variation in the vicinity of the pseudo-critical point, thus may lead to large buoyancy effect and flow pattern change in the near wall region and finally result in abnormal heat transfer behavior compared to conventional conditions.

In order to design supercritical fossil power plants, heat transfer experiment about supercritical water flowing in tubes has been performed since 1950s. These studies have been well reviewed by Cheng and Schulenberg [2] and Pioro and Duffy [3]. In the existing SCWR concepts [1, 4-5], various geometries of fuel assembly and different kinds of spacer grids were proposed. Most experimental work was performed for tube and annuli while only very few for rod bundles.

Dyadyakin and Popov [6] conducted experiments with a tight-lattice 7-rod bundles and observed significant pressure oscillations at large mass fluxes and high heat fluxes. Silin [7] reported that no heat transfer deterioration was observed in the experiments of supercritical water flowing inside multi-rod bundles within the test parameters range at which heat transfer deterioration occurred in tubes. Razumovskiy [8] investigated heat transfer of supercritical water in vertical 3-rod and 7-rod bundles for upward flow. The heat transfer deterioration was observed at certain heat flux, and the temperature peak moved to the beginning of the rod as the heat flux increased.

In most of the SCWR design concepts, spacer grids [9-11] or wires [5, 12-13] are proposed to position the fuel pins. In addition, spacers are also used to improve heat transfer. In spite of the significant effect of spacers on heat transfer, investigation on spacer effect is still very limited, especially in rod bundles at supercritical pressure conditions.

Based on the investigation to heat transfer of rod bundles in subcritical condition, Yao [14] developed a correlation to describe the heat transfer enhancement and its decay behavior downstream of spacer grids.

Miller [15] conducted experiments of heat transfer in 7x7-rod bundle under subcritical conditions. They founded that heat transfer enhancement reaches highest level just at the exit of the spacer and the heat transfer enhancement downstream the spacer decays along with distance. Both the maximum heat transfer enhancement and the decay procedure depend on Reynolds number.

Moon [16] conducted heat transfer experiments in a 6x6-rod bundle of single-phase steam flow. Heat transfer enhancement was found in both upstream and downstream of spacer grids. In the downstream of the spacer, heat transfer enhancement decays exponentially with the distance from the spacer grid. Their experimental data also showed that the Reynolds number affects the heat transfer enhancement only at low Reynolds number range.

Taking all the existing studies into consideration, it is concluded that further experimental investigations on heat transfer characteristics of supercritical water flowing in rod bundles with spacers are required. This paper presents experimental and numerical studies on heat transfer of supercritical water flowing upward in 2×2 rod bundles with spacer grids. The geometric parameters, e.g. hydraulic diameter, of the test section corresponded to those of

SCWR design, i.e. the diameter of the heated rod is 8 mm, P/D ratios are 1.18 and 1.3, resulting in hydraulic diameters of 4.6mm and 7.6 mm, respectively. Spacer grids with interval ranging from 200 mm to 400 mm are applied. These intervals are sufficiently large for the redevelopment of flow and heat transfer downstream the spacers, so that heat transfer coefficients with negligibly small effect of spacers can be obtained.

2. Experimental facility

Heat transfer experiments were performed at the SWAMUP test facility, shown in Figure 1. The SWAMUP facility consists of the main test loop, a cooling water loop, a water purification loop, and I&C system. The main test loop, consisting of a circulating pump, pre-heater, mixing chamber, two heat exchangers, accumulator and test sections, and is constructed for pressure up to 30 MPa, temperature up to 550°C, mass flow rate up to 1.3 kg/s and electrical power up to 1.2 MW. The main technical parameters are listed in Table 1.

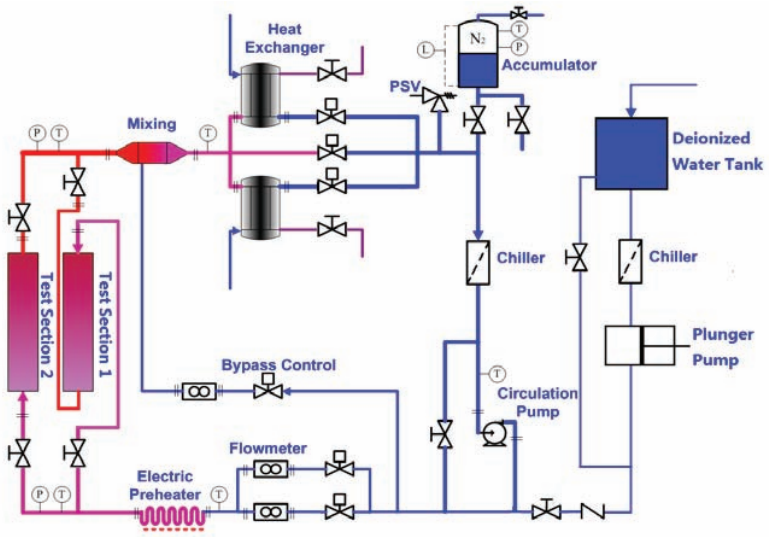

Figure.1: Scheme of the SWAMUP test facility

Table 1: Technical specification of the SWAMUP test facility

Parameters	Values	Units
Design pressure	30	MPa
Design temperature	550	°C
DC power for test section	0.9	MW
Heating power for pre-heater	0.3	MW
Heat exchanger capacity	1.2	MW
Max. flow rate	5.0	t/h
Pump head at maximum flow rate	80	m

3. Test section

The test section, as shown in Figure 2, consists of four Inconel 718 heated tubes (8 mm OD and 1.5 mm thickness) and a ceramic square tube (20.32×20.32mm and 23.2 ×23.2mm thickness), forming hydraulic diameters of 4.6mm and 7.3mm, respectively. The bundle has a length of the channel is 1328 mm and is supported by 5 or 6 space grids. The inside of heating tube is installed with a sliding thermal couple to measure the inner wall temperature. The outer square tube is unheated and covered with fiberglass insulation to minimize heating loss.

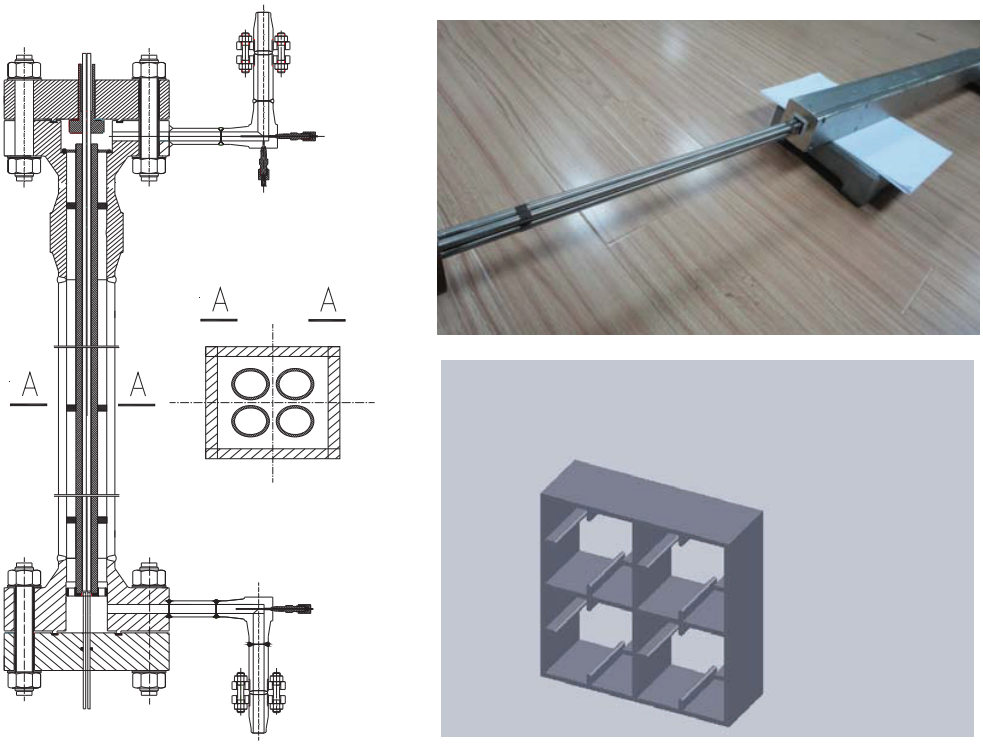

Figure.2 Schematic Diagram of Test Section and Space Grid

In order to measure 4 heated rods inside temperature, 4 sliding thermal couples were used. Each circumferential position of thermal couples is shown in Fig.3. During experiments, slide thermal couples are moved axially. Also, the 4 sliding thermal couples can also move circumferentially.

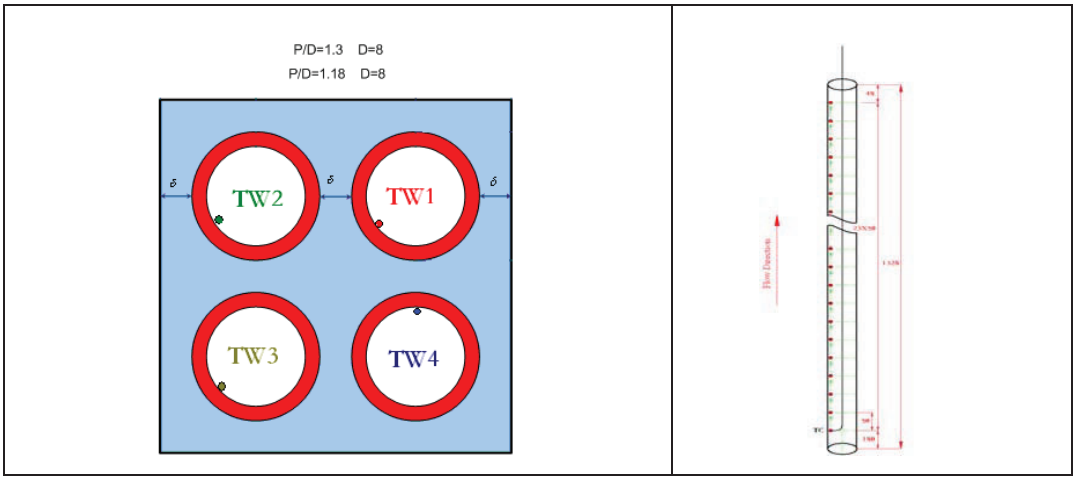

Figure.3: Circumferential position of sliding thermal-couples

4. Data reduction

Experiments were carried out with test parameters shown in Table 2. More than 500 measurement points were recorded. Temperatures on heating tube outside surface were calculated from the inner surface temperatures of the hated tube. It was assumed that the volumetric power density in the tube is uniform. Neglecting the axial heat conduction, one-dimensional heat conduction equation is numerically solved, so that outer wall temperatures were obtained. In the calculation, the temperature dependence of tube wall thermal conductivity was considered. The uncertainties of every parameter were shown in Table 3.

Table 2 Ranges of Test parameters

Parameters	Values	Units
Pressure	23, 25, 26	MPa
Mass flow rate	500-1500	kg/m^2s
Heat flux	0.40-1.50	MW/m^2
Bulk temperature	310-390	^{O}C

Table 3 Uncertainties of primary parameters

Parameters	Maximum uncertainty
Pressure	$\pm$ 0.2%
Mass flow rate	$\pm$ 0.4%
Fluid temperature	$\pm$ 1.5^{O}C
DC current	$\pm$ 1.0%
DC voltage	$\pm$ 1.0%
Heated tube diameter	$\pm$ 0.04mm
Heated tube thickness	$\pm$ 0.02mm

With the measured DC voltage, U, current, I, and thermal efficiency η, heat flux on the surface of the tubes can be calculated as following:

$$q_s = \frac{U \cdot I}{\pi D_o L}\eta \tag{1}$$

Taking the conservation of energy into consideration, the bulk specific enthalpy can be calculated with the inlet fluid enthalpy, H_{in}, and mass flow rate, G.

$$H(z) = H_{in} + \frac{4zq_s}{GA_{flow-channel}} \tag{2}$$

The outside wall temperature is iteratively calculated with

$$T_{wo} = T_{wi} + \frac{q_v}{4k_w}\left[\left(\frac{D_o}{2}\right)^2 - \left(\frac{D_i}{2}\right)^2\right] - \frac{q_v}{2k_w}\left(\frac{D_o}{2}\right)^2 \ln(\frac{D_i}{D_o}) \tag{3}$$

Where a uniform heating power density in the tube wall is assumed as

$$q_v = \frac{4U \cdot I}{\pi(D_o^{\,2} - D_i^{\,2})L}\eta \tag{4}$$

Finally, the bundle average heat transfer coefficient can be calculated with:

$$HTC_{ave} = \frac{q_s}{T_{wo}(z) - T_{b-ave}(z)} \tag{5}$$

Two different approaches are used to calculate the bulk fluid temperature, which is needed to calculate heat transfer coefficient. The first approach applies the bundle average fluid temperature, as shown in Eq.(5), whereas the second approach uses the sub-channel averaged fluid temperature, which is not measured, but determined by using CFD. The sub-channel based heat transfer coefficient can be calculated with:

$$HTC_{sub} = \frac{q_s}{T_{wo}(z) - T_{b-CFD}(z)} \tag{6}$$

5. Results and discussion

5.1 Wall temperature

Fig. 4 shows the wall temperature measured by 4 thermal couples in 3 kinds of sub-channels and rod gaps versus the distance from the test section entrance for the test condition: P=23 MPa, G=900 kg/m^{2}s and q=1.2 MW/m^2. It is seen that in downstream of spacer grids, heat transfer is enhanced and heated rod wall temperature decreases. Four thermal couples representing different sub-channels show similar temperature profile and the wall temperatures in center sub-channel are the lowest, in corner sub-channel are the highest.

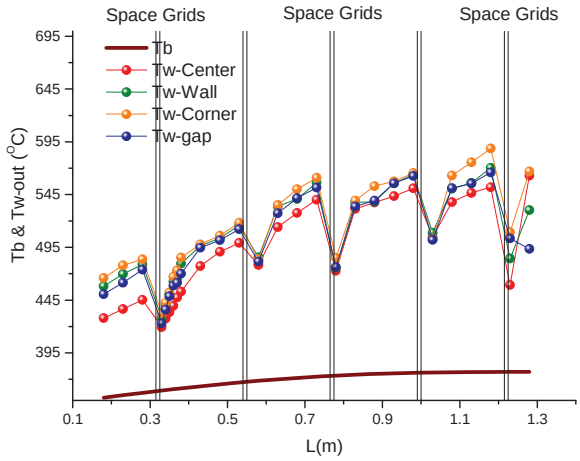

Figure.4 Heated wall temperature and average fluid temperature along axial position (P=23 MPa, G=900 kg/m^{2}s and q=1.2 MW/m^2)

In order to obtain the average fluid temperature in sub-channels, CFD method was used to simulate the heat transfer behavior of super-critical water for three different sub-channels. The computational domain is 1/4 of the bundle due to symmetry. Fig.5 shows the cross-section of computational domain and boundary conditions. For the axial direction, the computational domain includes 300 mm unheated part and 1328 mm heated length of the test section. Spacer grids were also created at both the fluid sub-domain and the solid sub-domain, as shown in Fig. 6(b).The near wall meshes were refined so that y+ values of the near wall meshes are smaller than 15, shown in Fig.6(a). The convergence criterion for normalized residual of each individual equation is set to be less than 10^{-5} and the mesh independence

were carefully checked. The Reynolds stress model of Speziale (SSG) [17] was used in the present simulation.

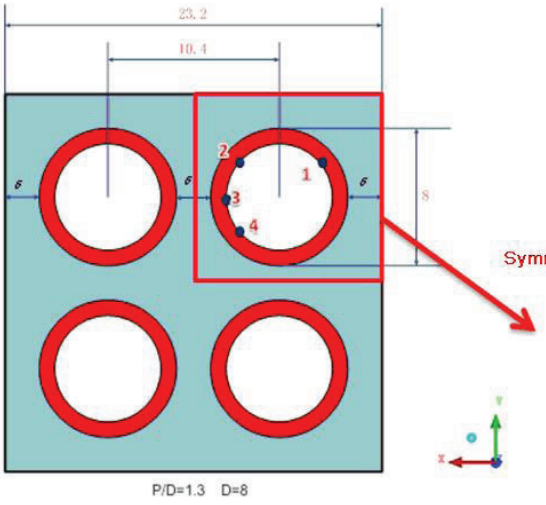

Figure 5(a) Cross section of rod bundles

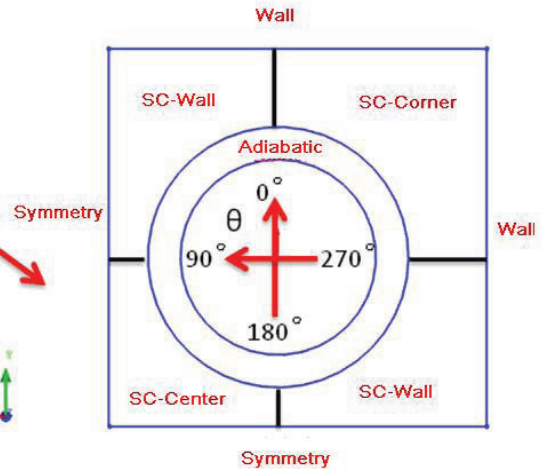

Figure 5(b) Simulation domain boundary condition

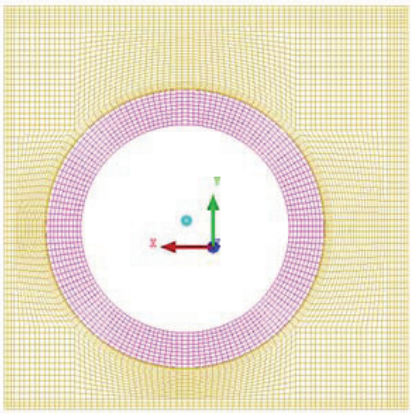

Figure. 6(a) Mesh for cross section

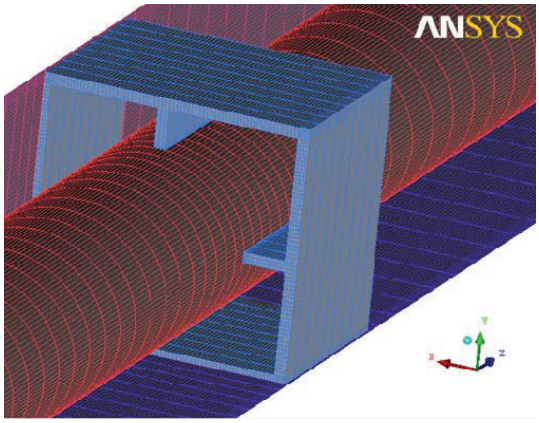

Figure. 6(b) Mesh for space grid

Fig.7 shows the comparison of wall temperature obtained from CFD and from the experiment versus axial positions at the condition of P=23MPa G=1000kg/m^2.s Q=0.8MW/m^2. It can be seen that the effect of spacer can be well predicted by CFD and the simulation results show a very good agreement with the experiment data.

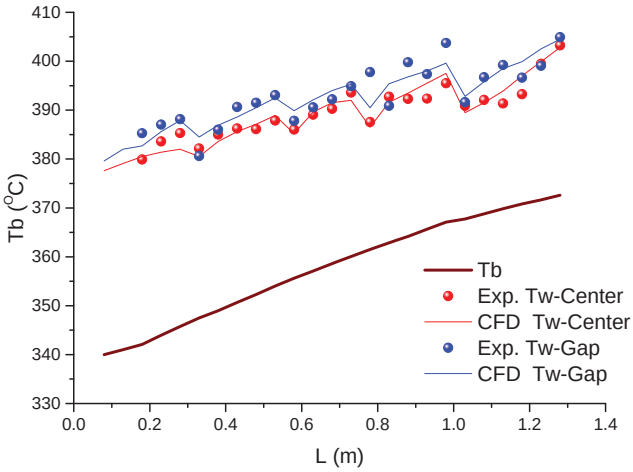

Figure.7 Temperature profile at center sub-channel and gap region

Fig.8 Shows the comparison of wall temperature obtained from CFD and from the experiment versus circumferential angels shown in Fig. 5(b) at the condition of P=23MPa G=1000 kg/m^2.s Q=1.0MW/m^2 Z=550 mm. It can be seen that the CFD simulation can predict the tendency but still a considerable deviation from the experiment data.

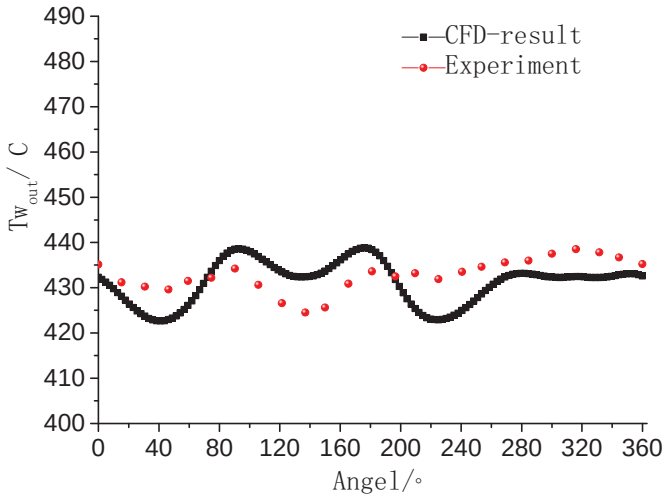

Fig.8 Wall temperature versus circumferential angels

Based on the CFD simulation, average fluid temperature in every sub-channel can be obtained. Thus, heat transfer coefficient conducted by sub-channel fluid temperature can be conducted. Fig.9 shows an example of comparison of heat transfer coefficient based on average cross section fluid temperature from energy balance and average sub-channel fluid temperature from CFD at the condition of P=25MPa, G=800kg/m^2.s,Q=0.8MW/m^2,P/D=1.3.

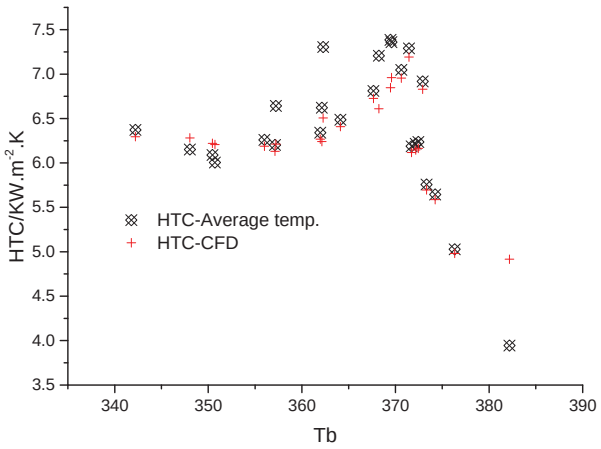

Figure.9 Comparison of HTC based on average bulk temperature and CFD center sub-channel fluid temperature

5.2 Heat transfer coefficient

Figure 10 shows the bundle average heat transfer coefficient versus the distance from the test section entrance for the test condition of Fig.4. Fig.10a presents the HTC distribution over the entire heated length and Fig. 10b presents the HTC distribution of center sub-channel in the axial position between two spacer grids. It is seen that just after the spacer grids, heat transfer coefficient increases strongly. With the increase in the downstream distance from the spacers, heat transfer coefficient decreases at first sharply and then smoothly. Far away from the upstream spacers, e.g. 40 times of the hydraulic diameter (Fig.10b), heat transfer coefficient approaches to a constant value. It can be concluded that at distance of more than 40 times hydraulic diameter, the effect of spacer on heat transfer coefficient is negligibly small. This conclusion is valid for all test conditions.

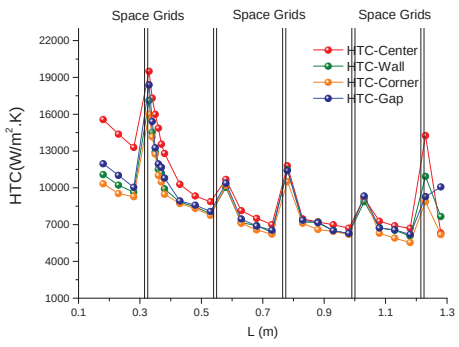

(a) Total heated length

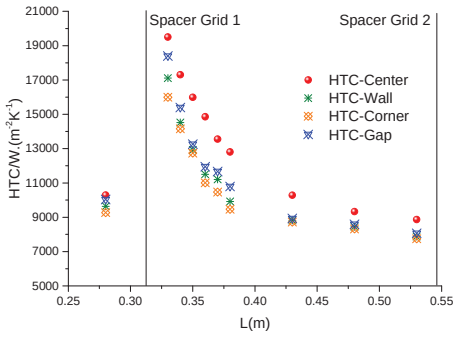

(b) Between two spacers

Figure 10: Average heat transfer coefficient along axial position (P/D=1.3, P=23 MPa, G=900 kg/m^{2}s and q=1.2 MW/m^2)

In the sub-chapter of 5.2, only test data with negligibly small effect of spacer grids are selected, i.e. the distance from the upsteam spacer grid is large than 40 times of hydraulic diameter. Figure 11 shows the sub-channel averaged HTCs in center sub-channel versus bulk temperature at two different pressures with the same mass flux and heat flux. Generally, at the lower pressure, the peaks of HTC are slightly higher. This is because of higher peak of Prandtl number at the lower pressure. For the test data presented here, strong heat transfer reduction occurs at sub-channel temperature approaching the pseudo-critical values.

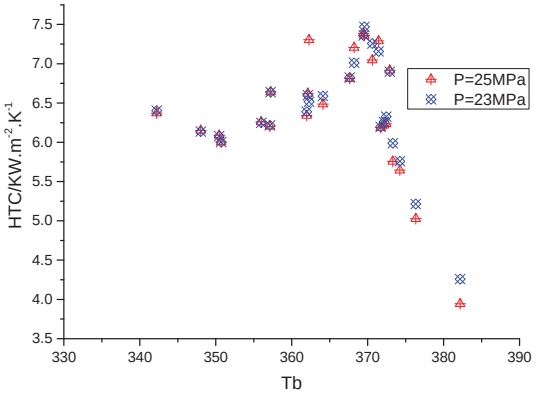

Figure.11 Effect of pressure on HTC (P/D = 1.3, G = 800 kg/m^{2}s, q = 0.8 MW/m^2)

Figure 12 shows the sub-channel average heat transfer coefficient in center sub-channel versus the bulk temperature at various heat fluxes. The pressure is 25 MPa, mass flux 800 kg/m^{2}s. The bulk temperature ranges from340°C up to 385°C. The effect of heat flux on heat transfer coefficient is small.

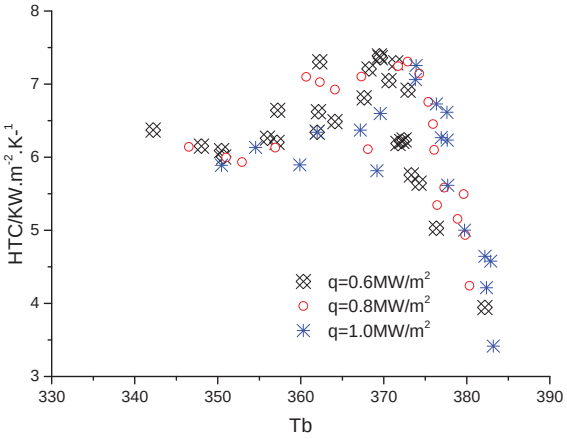

Figure.12 Effect of mass flux on HTC (P/D=1.3, P=25MPa,G=800kg/m^2.s)

Figure 13 shows the effect of mass flux on HTCs in center sub-channel. It is seen that higher mass flux leads to higher heat transfer coefficients. In the study with rod bundles, the effect of mass flux is stronger than in circle tube [18].

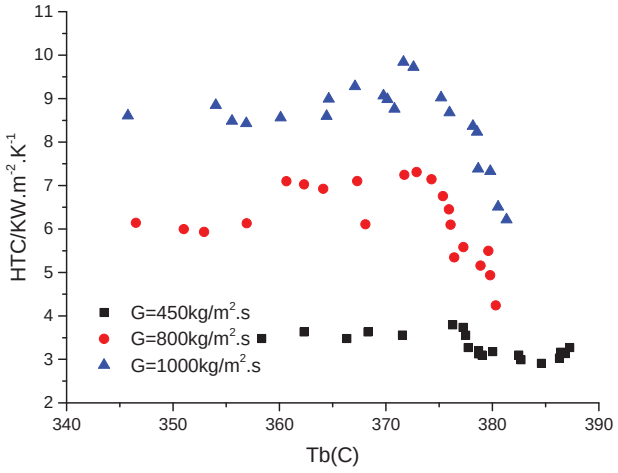

Figure.13 Effect of mass flux on HTC ((P/D=1.3, P=25MPa,q=0.8MW/m^2)

6. Conclusions

Experimental studies on heat transfer of supercritical water flowing in 2×2 rod bundles with spacer grids were performed at the SWAMUP test facility of SJTU with the following conditions: pressure from 23MPa to 26MPa, mass flux from 500-1500 kg/m^{2}s, heat flux from 0.4-1.5 MW/m^2 and bulk temperature from 310°C to 390°C. The test data were analyzed related to the effect of spacer grids, pressure, mass flux and heat flux. In addition, CFD simulations were carried out to investigate the flow and temperature distribution inside the rod bundle. Related to surface temperature of heated rods CFD results were compared with the experimental data. The following main conclusions can be achieved:

(1) The slide thermocouple technique enables the detailed analysis of the spacer effect on heat transfer and temperature circumferential profile.

(2) The strongest enhancement of heat transfer occurs at the exit of the spacer and the heat transfer enhancement decays with the distance from the spacer.

(3) Heat transfer coefficients are strongly affected by mass fluxes and spacers but barely affected by heat flux and pressure.

(4) Strong non-uniformity of heat transfer is obtained both in experiment and in numerical simulation. HTC in center sub-channel shows higher values than those in other circumferential positions.

(5)Two different methods to get HTC based on average bulk fluid temperature and fluid temperature obtained by CFD sub-channel were proposed.

Acknowledgement

The authors would like to thank China Nuclear Power Technology Research Institute for providing the financial and technology support for this study.

Reference

1. X. Cheng, X.J. Liu , Y.H. Yang, A mixed core for supercritical water-cooled reactor. Nucl. Eng. and Technol., 40, 117-126 (2008).

2. X. Cheng, T. Schulenberg, Heat transfer at supercritical pressures-Literature review and application to a HPLWR. Forschungszentrum Karlsruhe, Technik und Umwelt, Wissenschaftliche Berichte, FZKA 6609, Institute fur Kernund Energietechnik (2001).

3. I.L. Pioro, R.B. Duffey, Experimental heat transfer in supercritical water flowing inside channels (Survey). Nucl. Eng. Des. 235,2407–2430 (2005).

4. Y. Oka, S. Koshizuka, Design concept of one-through cycle supercritical pressure light water cooled reactor, in: Proc. of SCR-2000, Nol.6-8, Tokyo (2000).

5. T. Schulenberg, J. Starflinger, J. Heneche, Three pass core design proposal for a high performance light water reactor. Prog. Nucl. Energy, 50, 526-531. (2008).

6. B.V. Dyadyakin, A.S. Popov, Heat transfer and thermal resistance of tight seven-rod bundle, cooled with water flow at supercritical pressures. Trans. VTI (11), 244–253 (in Russian). (1977).

7. V.A. Silin, V.A. Voznesensky, A.M. Afrov, The light water integral reactor with natural circulation of the coolant at supercritical pressure B-500 SKDI. Nucl. Eng. Des. 144, 327–336. (1993).
8. V.G. Razumovskiy, E.N. Pismennyy, A.E. Koloskov, I.L. Pioro, Heat transfer to supercritical water in vertical 7-rod bundle. Proc. 16th Int. Conf. Nucl. Eng. ICONE-16 (2008).
9. X. Cheng, T. Schulenberg, D. Bittermann, P. Rau, Design analysis of core assemblies for supercritical pressure conditions, Nucl. Eng. Des. 233, 279-294 (2003).
10. K. Dobashi, Y. Oka, S. Koshizuka, Conceptual design of a high temperature power reactor cooled and moderated by supercritical light water. ICONE6, May 10–15, (1998).
11. D. Squarer, Y. Oka, D. Bittermann, N. Aksan, C. Maraczy, R. Kyrki-Rajamäki, A. Souyri, P. Dumaz, High Performance Light Water Reactor (HPLWR) FISA, Luxembourg, November (2001).
12. Y.Y. Bae, H.K. Joo, J. Jang, J. Song, H.Y. Yoon, "Research of a Supercritical Pressure Water Cooled Reactor in Korea", Proc. of ICAPP'04, Pittsburgh, Pa, USA, June 13-17(2004).
13. P. McDonald, J. Buongiorno, J.W. Sterbentz, C. Davis, R. Witt, "Feasibility Study of Supercritical Light Water Cooled Reactors for Electric Power Production", INEEL/EXT-04-02530, INEEL, January (2005).
14. S. Yao, L. Hochreiter, W. Leech, Heat transfer augmentation in rod bundles near grid spacers. J. Heat Transfer 104, 76–81 (1982).
15. D.J. Miller, F.B. Cheung, S.M. Bajorek, On the development of a grid-enhanced single-phase convective heat transfer correlation. Nuclear Engineering and Design 264, 56-60 (2013).
16. S. K. Moon , S. Cho, J. Kim, B. J. Kim, J. K. Park, Y. J.Yun, Enhancement of single-phase convective heat transfer in rod bundles near spacer grids. The 15th International Topical Meeting on Nuclear Reactor Thermal - Hydraulics, NURETH-15 NURETH15-505, Pisa, Italy, May 12-17 (2013).
17. C. Speziale, Modelling the pressure–strain correlation of turbulence: an invari-ant dynamical systems approach, Journal of Fluid Mechanics 277,245–272 (1991).
18. M. Zhao, H.Y. Gu, X. Cheng, Experimental study on heat transfer of supercritical water flowing downward in circle tubes. Annals of Nuclear Energy, 63, 339-349 (2014).